Liquid Crystals
Publication details, including instructions for authors and subscription information:
http://www.informaworld.com/smpp/title~content=t713926090

Effect of magnitude of dielectric anisotropy of a liquid crystal on light efficiency in the fringe-field switching nematic liquid crystal cell

Je Woo Ryu [a]; Ji Youn Lee [a]; Hyang Yul Kim [a]; Ji Woong Park [a]; Gi-Dong Lee [b]; Seung Hee Lee [a]
[a] Polymer BIN Fusion Research Center, School of Advanced Materials Engineering, Chonbuk National University, Chonju, Chonbuk 561-756, Korea
[b] Department of Electronics Engineering, Dong-A University, Pusan 607-735, Korea

Online Publication Date: 01 April 2008

To link to this article: DOI: 10.1080/02678290801919659
URL: http://dx.doi.org/10.1080/02678290801919659

Liquid Crystals,
Vol. 35, No. 4, April 2008, 407–411

Effect of magnitude of dielectric anisotropy of a liquid crystal on light efficiency in the fringe-field switching nematic liquid crystal cell

Je Woo Ryu[a], Ji Youn Lee[a], Hyang Yul Kim[a], Ji Woong Park[a], Gi-Dong Lee[b] and Seung Hee Lee[a]*

[a]*Polymer BIN Fusion Research Center, School of Advanced Materials Engineering, Chonbuk National University, Chonju, Chonbuk 561-756, Korea;* [b]*Department of Electronics Engineering, Dong-A University, Pusan 607-735, Korea*

(Received 2 December 2007; final form 15 January 2008)

The light efficiency of most well-known nematic liquid crystal (LC) modes, such as twisted nematic and in-plane switching, depends only on the cell retardation value, irrespective of the cell gap and dielectric anisotropy of the LC. Interestingly, the light efficiency of a homogenously aligned nematic LC cell driven by a fringe electric field, termed the fringe-field switching (FFS) mode, is found to be dependent on the magnitude of dielectric anisotropy, such that an LC with high dielectric anisotropy results in lower light efficiency than that of an LC with low dielectric anisotropy.

Keywords: light efficiency; fringe-field switching; dielectric anisotropy; nematic LC cell

1. Introduction

Nowadays, liquid crystal displays (LCDs) are being used in all types of information displays. The image quality of the LCDs has greatly improved in recent years due to the development of new liquid crystal (LC) modes, such as film-compensated twisted nematic (TN) (*1, 2*), in-plane switching (IPS) (*3, 4*), fringe-field switching (FFS) (*5–10*), and multi-domain vertical alignment (MVA) including patterned VA (PVA) (*11*). Although the image quality of the LCDs is greatly improved by these LC modes, their transmittance is quite poor, normally less than 10%, due to the use of an absorptive colour filter, polariser, limited aperture ratio and insufficient light efficiency by the LC layers. In LCDs, light modulation occurs either by phase retardation or a polarisation rotation effect using the LC layers. In general, the light efficiency of an LC cell depends only on the retardation, $d\Delta n$, of the LC layer, where d is the thickness of the LC layer and Δn is the birefringence of the LC, i.e. it remains unchanged as long as the retardation value is the same regardless of whether d or Δn is changed.

Among the wide-viewing-angle LC modes, both IPS and FFS modes, where the LCs are aligned homogeneously in the initial state and an in-plane and fringe electric field, respectively, rotates the LC almost in plane, can use LCs with positive or negative dielectric anisotropy ($\Delta\varepsilon$). In IPS mode, the light efficiency of the LC cell is not dependent on the dielectric anisotropy of the LC because the in-plane field drives the LC to rotate (*12*). However, in FFS mode, the light efficiency strongly depends on sign of the dielectric anisotropy of the LC because the LC above the electrode is tilted upward along the fringe-electric field line for a LC with a positive $\Delta\varepsilon$ (+LC), whereas the tilt angle for the LC with a negative $\Delta\varepsilon$ (−LC) is not so high (*13–15*). In addition, unlike in the other devices such as TN, IPS and MVA, the light efficiency of a LC cell is strongly dependent on the cell gap because the rotation angle of the LCs at the centre of the electrodes is determined by the rotating angle of the neighbouring molecules (*16, 17*).

Until now, LCDs employing FFS mode using both +LC and −LC have been commercialised but recent major products such as tablet PC, notebooks, monitors and LC-TV use +LC, on account of their low operating voltage and rapid response time. However, when using +LC, the light efficiency of the LC cell is slightly lower than the cell using the −LC cell. The light efficiency of the device is very important because it determines transmittance of the device associated with the cost and the brightness of the LCDs. This study reports the experimental and calculated results showing that the light efficiency of FFS mode depends on the magnitude of $\Delta\varepsilon$ of the +LC.

2. Switching principle of the FFS mode

In FFS mode, the LCs are aligned homogenously in the initial state with their optical axis coincident with one of the crossed polariser axes so that in the off state the cell appears black. Considering the electrode structure, a common electrode with a plane shape is located below the pixel electrodes of slit form, with a

*Corresponding author. Email: lsh1@chonbuk.ac.kr

ISSN 0267-8292 print/ISSN 1366-5855 online

DOI: 10.1080/02678290801919659
http://www.informaworld.com

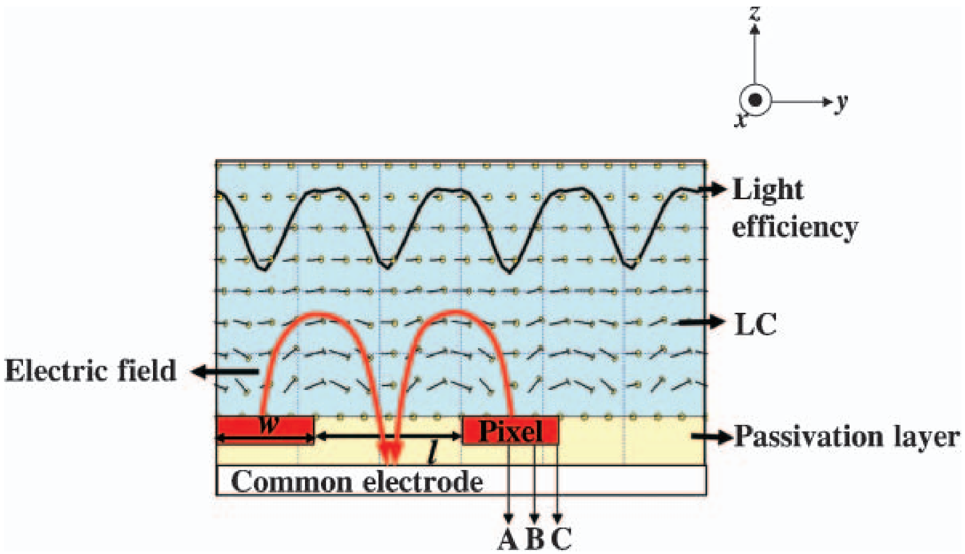

Figure 1. Configuration of the LC molecules and corresponding transmittance in the white state of the FFS mode using a +LC.

passivation layer between the pixel and common electrodes, as shown in Figure 1 (*5*). Here, the pixel electrode has a width (w) and a distance (l) between them. With a bias voltage, a fringe electric field with both horizontal (E_y) and vertical (E_z) components is generated, which rotates the LCs above the whole electrode surface, giving rise to transmittance.

The interesting feature of FFS mode is that the transmittance oscillates periodically along the electrodes, due to the different twist angle of the LC along the electrode position. At position C, where a strong E_y exists, the LC is twisted enough by a dielectric torque proportional to $|\Delta\varepsilon|\ E_y^2$, giving rise to high transmittance. The lower transmittance at the centre of the electrode (position A) than that at the edge of the electrode (position C), as well as between the centre and edge of the electrodes (position B), arises from the low twist angle compared with the other regions. According to previous studies (*16, 17*) there is no horizontal electric field to rotate the LC at position A so that the twist angle of the LC at that position is determined by the elastic torque of the neighbouring molecules (proportional to $\mathbf{n}_A \cdot \mathbf{n}_B(\mathbf{n}_A \times \mathbf{n}_B)$), where $\mathbf{n}_A$ and $\mathbf{n}_B$ represents the LC directors at position A and B, respectively) (*17*), particularly position B. In addition, with bias voltage, the LC reorientation at positions C and B does occur due to dielectric torque at first and then it does occur at position C due to elastic torque with neighbouring molecules. Because of this abnormal switching principle of the FFS mode, the transmittance at position A decreases with decreasing cell gap because more LCs are influenced by surface anchoring, i.e. surface anchoring overcomes elastic torque. Especially, when using the +LC, the LCs at position B tilt upward to some degree in response to fringe-field direction so that a lower elastic torque to twist the LC at position A is applied, giving rise to a relatively low transmittance compared with positions B and C. This means that the degree of tilt angle at position B strongly affects the twist angle of the LC at position A and can differ according to the magnitude of $\Delta\varepsilon$ of the +LC.

3. Results and discussion

Experiments and computer simulations were performed to determine if the transmittance is dependent on the magnitude of $\Delta\varepsilon$. In the experiments, the width of the pixel electrode and the distance between them was 4 µm and 6 µm, respectively. The thickness of the insulation layer was 6300 Å, and the cell gap was 3.6 µm. Two different types of LC, LC1 (Δn=0.098, clearing temperature T_{ni}=75°C, rotational viscosity γ=64 mPa s, $\Delta\varepsilon$=5 at 20°C, 1 kHz) and LC2 (Δn=0.0988, clearing temperature T_{ni}=92.5°C, rotational viscosity γ=108 mPa s, $\Delta\varepsilon$=9.4 at 20°C, 1 kHz) were selected because both had similar birefringence but the magnitudes of their dielectric anisotropy were significantly different. The simulations were performed using commercially available software LCD Master (Shintech, Japan), where the motion of the LC director was calculated based on the Ericksen–Leslie theory, and the 2×2 extended Jones matrix was used for the optical transmittance calculation (*18*). In the simulations, the same electrode structures as those in the experiment were applied and all the physical properties of LC1 and LC2 kept the same as each other except for $\Delta\varepsilon$. For simulations, the elastic constants of the LC, K_1, K_2 and K_3, are assumed to be 9.7 pN 5.2 pN, and 13.3 pN, respectively. In both the experiment and calculation, the rubbing angle was 80° with respect to the horizontal component of the fringe electric field with a pretilt angle of 2°.

Figure 2 shows the measured and calculated voltage-dependent transmittance (*V–T*) curves. Here, the transmittance is defined as average light efficiency along the whole electrode surface, *w+l*. As can be seen, the results show that the cell with LC1 has a better transmittance than that with LC2, i.e. the transmittance of the cell with $\Delta\varepsilon=5$ is approximately 6% higher than that with $\Delta\varepsilon=9.4$. Although the simulated results did not consider the difference of the LC elastic constants, both are in good agreement, implying that the transmittance difference comes mainly from the difference in magnitude of dielectric anisotropy. In addition, in the FFS mode with positive dielectric anisotropy, the optimal cell retardation value that provides maximal transmittance is close to 0.4 μm (*13*), i.e. the cell with LC2 should show a better transmittance than the cell with LC1 since Δn of the LC2 is slightly higher than that of the LC1. However, the result observed is the reverse of that expected.

In the experiments, the elastic constants of the two LCs were different; however, for simulations the same parameters were used and both results show consistently that the transmittance depends on the magnitude of dielectric anisotropy of the LC. On the other hand, the threshold voltage V_{th} in the cell with LC1 was higher than in the cell with LC2 because it is proportional to $(1/\Delta\varepsilon)^{1/2}$. In order to neglect the V_{th} difference in *V–T* curves, they were redrawn using a reduced voltage (V/V_{th}), as shown in Figure 3. Clearly, the maximum transmittance at the same reduced voltage is higher in the cell with LC1 than that with LC2.

To confirm the dependence of the transmittance on $\Delta\varepsilon$ in the FFS mode, the transmittance was calculated as a function of $\Delta\varepsilon$ of the +LC while keeping other physical parameter the same, as shown in Figure 4. The calculated results clearly show that the transmittance increases linearly with decreasing $\Delta\varepsilon$ of the +LC with a negative slope of 0.685.

Since the light efficiency in FFS mode with +LC is strongly dependent on the electrode position, the light efficiency above the pixel electrode for LC1 and LC2 was compared, as shown in Figure 5. The decreased light efficiency of LC2 arises from a decrease along the electrode between positions A and B, particularly at position A. As mentioned in section 2, the degree of twist angle of the LC determines light efficiency at these

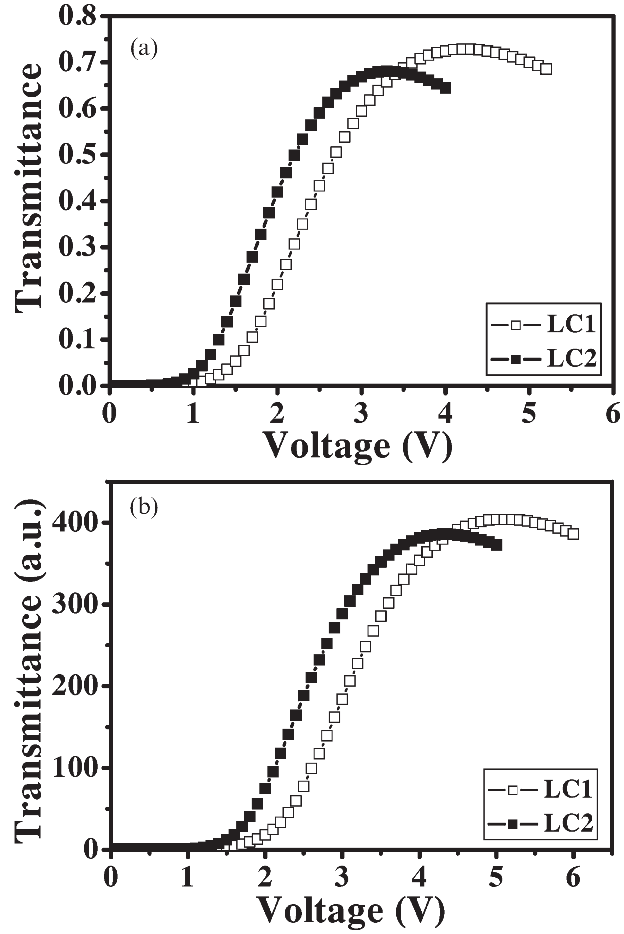

Figure 2. (a) Calculated and (b) measured voltage-dependent transmittance curves in the two different +LCs with different dielectric anisotropy, $\Delta\varepsilon$.

positions. In addition, the twist angle of the LC at position A is determined by orientation of LC at position B.

In order to understand this behaviour in more detail, the LC director profile along the LC layers was calculated at the same reduced voltage, as shown in Figure 6. An investigation of the tilt angle at position B revealed that both LC1 and LC2 have a similar orientation at low reduced voltages, i.e. 1.0, which is just V_{th} (see Figure 6(a)). However, at a reduced voltage of 1.7, which is higher than V_{th}, the maximum tilt angles for LC1 and LC2 are 13.7° and 16.0°, respectively, at $z/d=0.2$. With further increase of voltage close to the operating voltage with reduced voltage of 2.7, a difference in the tilt angle below mid-director exists, such that the maximum tilt angles for the LC1 and LC2 at $z/d=0.2$ are 33.0° and 35.4°, respectively. This is due to the stronger dielectric torque between the LC and E_z for LC2 than that for a LC1 on account of the higher dielectric anisotropy in the LC2 than in the LC1. Consequently, the different

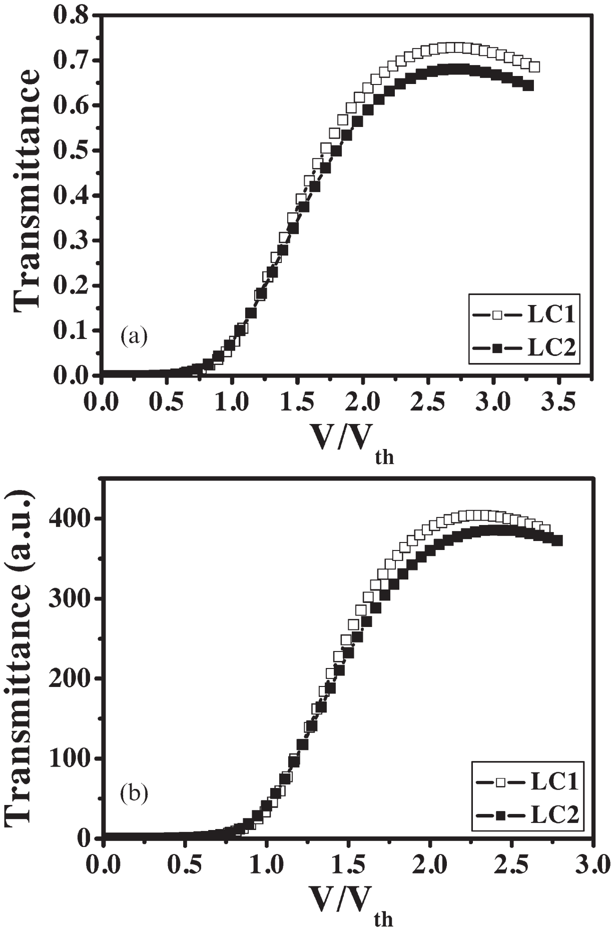

Figure 3. (a) Calculated and (b) measured transmittance curves in the two different +LCs according to the reduced voltage.

degree of tilt angle will bring up different twist angle at position A because the elastic torque to rotate the LCs above position A is determined by orientation of LC at position B. As a result, the maximum twist

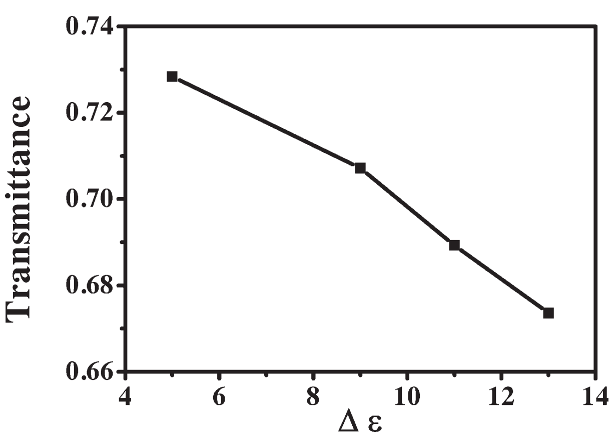

Figure 4. Transmittance as a function of the magnitude of $\Delta\varepsilon$ of the +LC.

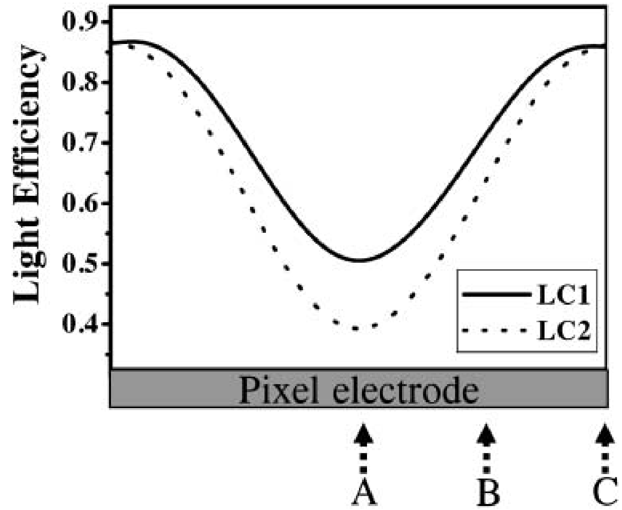

Figure 5. Calculated light efficiency above a pixel electrode as a function of the magnitude of $\Delta\varepsilon$ of the +LC.

angles from initial orientation for the LC1 and LC2 at $z/d=0.4$ with reduced voltage 2.7 are 29.3° (80°–50.7°) and 23.5° (80°–56.5°), respectively, at position A (see Figure 6(b)), i.e. it is less in LC2 than in LC1. At position A, the light efficiency of the cell is proportional to $\sin^2 2\Psi$, where Ψ is the angle between the LC director and the transmission axes of the crossed polarisers. Therefore, since Ψ in LC2 is smaller than that in LC1, the light efficiency of the cell with LC2 has a lower value than that of the cell with LC1, which is the origin for lower transmittance in the LC2 than that in the LC1.

4. Summary

In summary, this study examined the transmittance of the FFS mode in terms of the magnitude of positive dielectric anisotropy of the LC. Unlike conventional LC modes, such as TN and IPS modes, the transmittance depends on the dielectric anisotropy such that the transmittance increases with decreasing dielectric anisotropy of the LC. This unexpected behaviour in the FFS mode arises from the fact that the rotating angle of the LC is determined by the dielectric torque and elastic torque depending on the electrode positions. It is believed that this concept can be applied to the development of a LC for a high-performance FFS device.

Acknowledgements

This research was supported by a grant (F0004132) from Information Display R&D Center, one of the 21st Century Frontier R&D Programs funded by the Ministry of Commerce, Industry and Energy of the

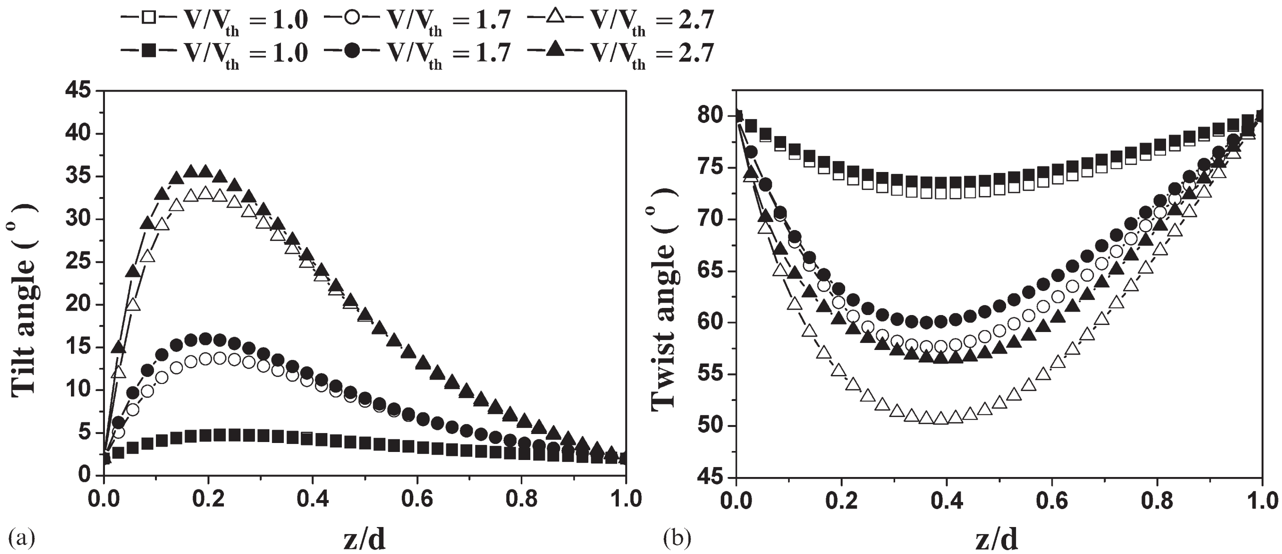

Figure 6. Reduced voltage-dependent LC (a) tilt angle at the electrode position between the centre and edge (position B), and (b) twist angle at the centre of the pixel electrode (position A) for two different LCs with different magnitude of $\Delta\varepsilon$. The filled and unfilled symbols indicate LC1 and LC2, respectively.

Korean government and partially supported by Merck Advanced Technology in Korea.

References

(1) Mori H. *J. Display Technol* **2005**, *1*, 179–186.
(2) Park C.H.; Jeong J.K.; Kim K.J.; Choi H.C.; Lee S.H. *Appl. Phys. Lett* **2006**, *89*, 101119.
(3) Oh-E M.; Kondo K. *Appl. Phys. Lett* **1995**, *67*, 3895–3897.
(4) Ohta M.; Oh-e M.; Kondo K., In *Asia Display'95* **1995**, pp. 707–710.
(5) Lee S.H.; Lee S.L.; Kim H.Y. *Appl. Phys. Lett* **1998**, *73*, 2881–2883.
(6) Lee S.H.; Lee S.L.; Kim H.Y., In *Asia Display '98* **1998**, pp. 371–374.
(7) Lee S.H.; Lee S.L.; Kim H.Y.; Eom T.Y. *Dig. Tech. Pap. Soc. Inf. Display Int. Symp* **1999**, 202–205.
(8) Lee S.H.; Lee S.M.; Kim H.Y.; Kim J.M.; Hong S.H.; Jeong Y.H.; Park C.H.; Choi Y.J.; Lee J.Y.; Koh J.W., et al. *Dig. Tech. Pap. Soc. Inf. Display Int. Symp* **2001**, 484–487.
(9) Lee S.H.; Kim H.Y.; Lee S.M.; Hong S.H.; Kim J.M.; Koh J.W.; Lee J.Y.; Park H.S. *J. Soc. Inf. Display* **2002**, *10*, 117–122.
(10) Takeda A.; Kataoka S.; Sasaki T.; Chida H.; Tsuda H.; Ohmuro K.; Sasabayashi T.; Koike Y.; Okamoto K. *Dig. Tech. Pap. Soc. Inf. Display Int. Symp* **1998**, 1077–1080.
(11) Kim K.H.; Lee K.; Park S.B.; Song J.K.; Kim S.N.; Souk J.H. *Asia Display* **1998**, 383–387.
(12) Oh-e M.; Yoneya M.; Kondo K. *J. Appl. Phys* **1997**, *82*, 528–535.
(13) Lee S.H.; Lee S.L.; Kim H.Y.; Eom T.Y. *J. Kor. Phys. Soc* **1999**, *35*, S1111–S1114.
(14) Jung S.H.; Kim H.Y.; Kim J.-.H.; Nam S.-.H.; Lee S.H. *Jap. J. Appl. Phys* **2004**, *43*, 1028–1031.
(15) Kim S.J.; Song I.S.; Lee S.H.; Kim H.Y.; Kim S.Y.; Lim Y.J. *Mol. Cryst. Liq. Cryst* **2006**, *449*, 87–94.
(16) Kim S.J.; Kim H.Y.; Lee S.H.; Lee Y.K.; Park K.C.; Jang J. *Jap. J. Appl. Phys* **2005**, *44*, 6581–6586.
(17) Jung S.H.; Kim H.Y.; Lee M.-H.; Rhee J.M.; Lee S.H. *Liq. Cryst* **2005**, *32*, 267–275.
(18) Lien A. *Appl. Phys. Lett* **1990**, *57*, 2767–2769.